Chapter 8

Exploring Membrane Lipid and Protein Diffusion by FRAP

Parijat Sarkar and Amitabha Chattopadhyay

Abstract

Knowledge of membrane dynamics is crucial since it allows us to understand membrane function. Fluorescence recovery after photobleaching (FRAP) is a widely used technique to monitor diffusion of lipids and proteins in biological membranes. We outline here general aspects of FRAP, followed by a step-by-step guide to carry out FRAP measurements for exploring diffusion of fluorescently labeled lipids and proteins in membranes of attached cells and membranes of *Candida albicans*. In this process, we have provided detailed hands-on tips, judicious use of which would ensure reliability and quality of acquired FRAP data and associated analysis.

Keywords FRAP, Confocal microscopy, Lateral diffusion, Mobile fraction, Diffusion coefficient, DiI, GFP

1 Introduction

Fluorescence recovery after photobleaching (FRAP) is one of the most widespread approaches for quantitative analysis of lateral diffusion characteristics in membranes [1–6]. Although the basic principles of FRAP (*see* [7] for a lucid description of the early history of FRAP) were developed almost four decades ago [8–12], the technique has experienced a resurgence due to the development of photostable fluorescence probes, generation of green fluorescent protein (GFP, see later), and rise of commercially available confocal microscopes [13, 14]. FRAP is a photoperturbation technique that involves generation of a concentration gradient of fluorescent molecules by irreversibly photobleaching (i.e., a photo-induced covalent modification of fluorophores that extinguishes its fluorescence) a fraction of fluorophores in a selected region. By making a fraction of fluorescent molecules invisible, FRAP alters the steady fluorescence intensity in a region of the cell without disrupting or creating any protein gradients. The dissipation of this fluorescence gradient with time occurs as the surrounding unbleached fluorescent molecules re-equilibrate in the bleached

Rajendra Prasad and Ashutosh Singh (eds.), *Analysis of Membrane Lipids*, Springer Protocols Handbooks,
https://doi.org/10.1007/978-1-0716-0631-5_8,

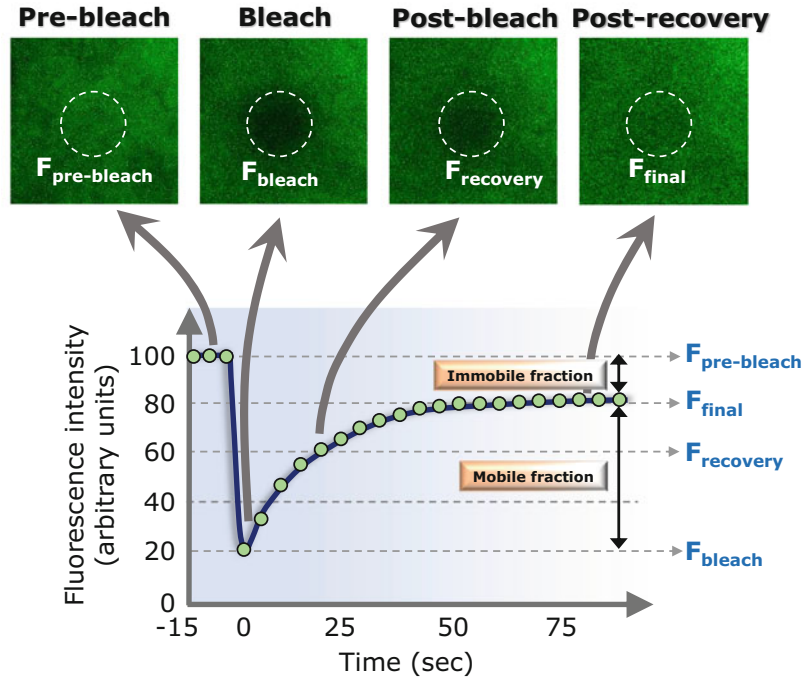

Fig. 1 The basic design of a FRAP measurement. The initial total fluorescence intensity in a region of interest (ROI) on the cell surface before photobleaching is denoted as $F_{\text{pre-bleach}}$. A concentration gradient of fluorescent molecules is generated by irreversibly photobleaching a population of fluorophores in the ROI (shown as a dashed circle) using a high-power laser beam. The total fluorescence intensity in the ROI immediately after photobleaching is shown as F_{bleach}. The concentration gradient of fluorophores gets dissipated with time due to lateral diffusion of unbleached fluorophores (outside ROI) into the bleached region and bleached fluorophores (inside ROI) away from the bleached region. The total fluorescence intensity in the ROI after complete fluorescence recovery is termed as F_{final}. Analysis of the rate of recovery of fluorescence (from F_{bleach} to F_{final}) yields the lateral diffusion coefficient (D). The extent of fluorescence recovery provides information on the fraction of molecules that are mobile in this time scale (termed mobile fraction, M_f)

region, which is then monitored (*see* Fig. 1). The extent and rate at which fluorescence recovery takes place can be quantified to describe the diffusion parameters. Two key diffusion parameters of a molecule can be obtained from quantitative FRAP measurements: the mobile fraction (M_f), which is the fraction of molecules that can diffuse into the bleach region during the time course of the measurement, and the diffusion coefficient (D) that reflects the rate of molecular movement. Analysis of FRAP measurements therefore provides information on the diffusion characteristics of an ensemble of molecules, as the area monitored is large and typically in the order of micrometers [15].

Lateral diffusion in biomembranes is a fundamental biophysical process that regulates the dynamics of lipid–protein and protein–protein interactions at the cell surface [16]. Lateral diffusion of receptors in the membrane represents an important determinant of

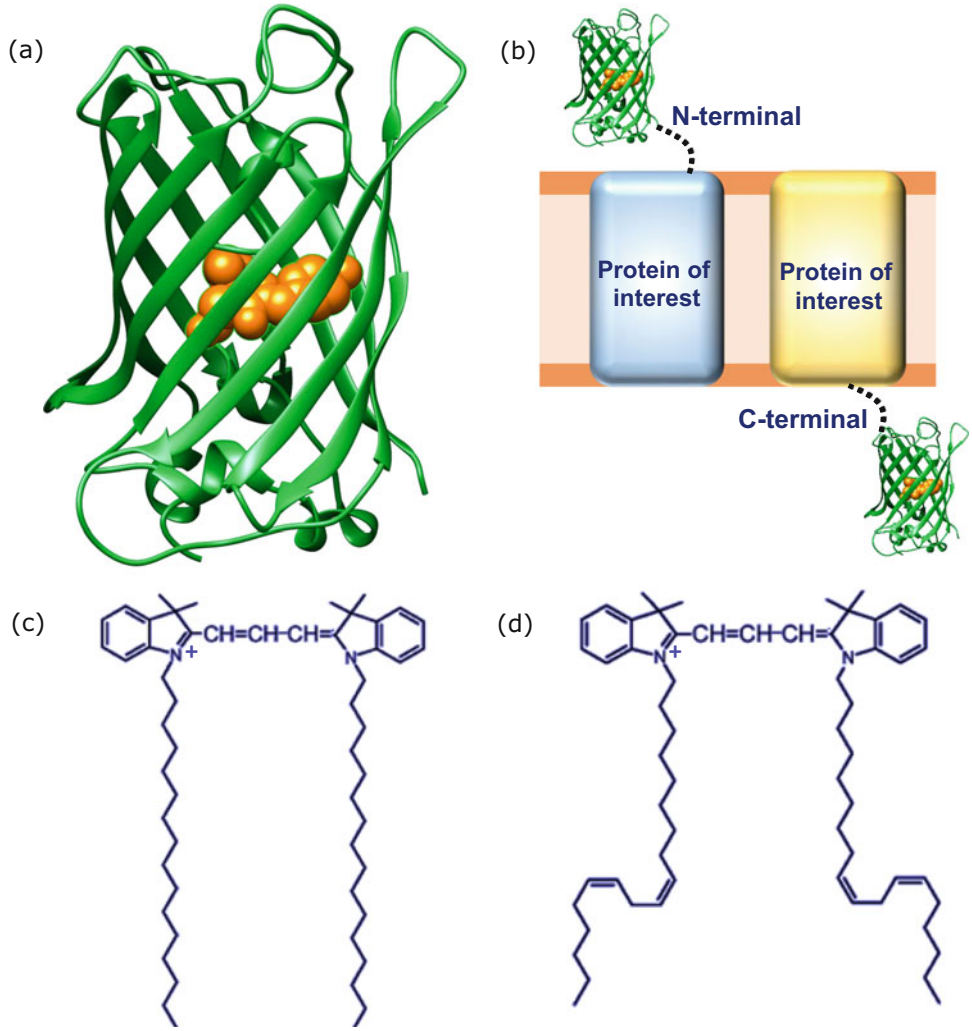

Fig. 2 Chemical structures of common fluorescent probes used for measuring membrane dynamics using FRAP. (**a**) The crystal structure of green fluorescent protein (GFP) that has been most widely used in the context of studying lateral diffusion of membrane proteins. As shown in panel (**a**), GFP has a β-barrel structure with the chromophore (an amino acid triplet (Ser–Tyr–Gly), highlighted in orange) located in the core of the protein. Molecular graphics was generated using UCSF Chimera package (https:/www.cgl.ucsf.edu/chimera) from the PDB entry 1EMB. (**b**) GFP can be attached at either the N- or C-terminal of virtually any protein of interest, and it can still fold into a fluorescent molecule. The resulting GFP-tagged protein could be used to study protein dynamics. (**c**) $DiIC_{18}(3)$ and (**d**) *FAST* DiI are common fluorescent probes used to quantify lipid dynamics in membranes

the overall efficiency of the signal transduction process [17]. In this context, GFP and its variants have become popular reporter molecules for monitoring expression, localization, and mobility of various membrane proteins by tagging it to the N- or C-terminal of the protein of interest [18–22] (Fig. 2). The use of GFP-tagged proteins to study membrane dynamics has a number of advantages:

(1) cellular transcription and translation ensure the presence of receptors covalently attached to fluorescent proteins in cells and eliminate the necessity of labeling receptors with fluorescent ligands before each experiment, (2) the stoichiometry of the receptor and fluorescent protein is well defined as the latter is covalently attached to the receptor at the DNA level, (3) complications encountered while using fluorescent ligands such as dissociation of ligands are avoided, and (4) analysis of unliganded states of the receptor becomes possible, which is otherwise not permitted with fluorescently labeled ligand. Another remarkable aspect of GFP fusion is that in spite of its large size (~27 kDa), most (but not all, *see* [23]) proteins maintain their native biochemical and pharmacological characteristics after fusion with GFP (or its variants). Importantly, the physical principles that define the diffusion of molecules in membranes are different from that of molecules diffusing in a bulk solvent. This is due to the fact that lateral diffusion in the membrane is relatively insensitive to size of the diffusing molecule since the diffusion coefficient is proportional to the logarithm of the reciprocal of the hydrodynamic radius of the diffusing molecule [22, 24]. As a consequence, unlike diffusion of soluble proteins in the cytoplasm, the size dependence of the diffusion of membrane proteins is rather subtle, and in spite of relatively large size of the GFP tag (~27 kDa), its effect on diffusion parameters is minimal.

Fluorescently labeled lipid analogs are widely used for measuring lateral dynamics of lipids in membranes [25, 26]. The DiI group of lipids are well characterized and commonly used probes for such measurements. They are composed of a polar indocarbocyanine headgroup and two hydrophobic alkyl chains (*see* Fig. 2c, d) that impart an overall amphiphilic character. These probes have earlier been shown to preferentially partition into fluid (disordered) or gel (ordered) phases of the membrane depending on the degree of similarity between their acyl chain length and those of lipids that comprise the host plasma membrane [27–29]. $DiIC_{18}(3)$ and *FAST* DiI (Fig. 2c, d) represent two such probes having similar intrinsic fluorescence characteristics but differing in their membrane phase partitioning preference. Fluorescence quenching analysis has earlier shown that $DiIC_{18}(3)$ prefers to partition into a more ordered phase [27, 28]. *FAST* DiI, on the other hand, is expected to partition more into disordered regions of the plasma membrane due to unsaturation in its acyl chains that would introduce kinks in the acyl chain leading to packing defects in the membrane [26, 30]. This is further supported by the observed similarities in endosomal trafficking properties of *FAST* DiI with short-chain DiI analogs [31] that are known to preferentially partition into a more disordered phase of the membrane [28]. Importantly, we previously showed that $DiIC_{16}(3)$ (a probe similar to $DiIC_{18}(3)$) displays a significant extent of detergent insolubility (a property of ordered membrane domains) relative to *FAST* DiI

in cell membranes, which possibly could reflect partitioning preferences of these probes into different membrane domains [29]. We previously analyzed lateral diffusion characteristics of DiI group of fluorescent lipids in natural membranes using FRAP [32]. In another study, *FAST* DiI was used to monitor lipid diffusion in membranes of the wild type and mutants lacking ergosterol of the pathogenic yeast *Candida albicans* [33]. Interestingly, by measuring lipid diffusion in *C. albicans*, we demonstrated that lipid dynamics in membranes of the wild type and ergosterol biosynthetic mutants of *C. albicans* correlates well with their drug resistance characteristics.

In this protocol, we focus on FRAP measurements to assess plasma membrane dynamics utilizing fluorescent lipid analogs and fluorescently labeled proteins. We describe here basic principles of FRAP measurements, time-lapse imaging, bleaching, and recovery of fluorescence with an emphasis on compulsory controls and finally discuss some aspects of data processing.

2 Materials

(a) Solvents and buffers.
   (i) Freshly prepared 1 M sorbitol, 0.1 M EDTA buffer (buffer A).
   (ii) Spectroscopy grade methanol and ethanol.
   (iii) Phosphate buffer saline (PBS; pH 7.4).

(b) Reagents.
   (i) Stock solution of $DiIC_{18}(3)$ and *FAST* DiI in spectroscopy grade methanol (*see* **Note 1**).
      • Measure the stock concentration using the molar extinction coefficient of 148,000 M^{-1} cm^{-1} at 549 nm [32].
   (ii) Poly-L-lysine (0.01% w/v) in Milli-Q water.
   (iii) Glass coverslip (22 mm); thickness 0.17 mm or commonly known as #1.5 coverslips (*see* **Note 2**).

3 Methods

(a) *Labeling of adherent cells.*
   (i) Grow cells on Lab-Tek chamber slides under the required experimental conditions.
   (ii) Wash twice in cold PBS before labeling them with fluorescent lipid probes.

(iii) Label the plasma membrane of cells using 15 μM (final concentration) *FAST* DiI for 30 min or 8 μM (final concentration) $DiIC_{18}(3)$ for 60 min at 4 °C.
- Stock solutions of the DiI probes are diluted in PBS to prepare the labeling solutions making sure that the residual methanol concentration is always <0.1% (v/v).
- In case of analysis of lateral diffusion of membrane proteins, skip **Steps (ii)** and **(iii)**, and use a suitable cell line expressing the fluorescently tagged protein of interest (*see* **Note 3**).

(iv) Labeled cells are washed twice in PBS.

(v) FRAP measurements are performed on cells in PBS containing 1 mM $CaCl_2$ and 0.5 mM $MgCl_2$.

(b) *Labeling of yeast/Candida cells.*

(i) Suspend an overnight grown culture of cells at a density of ~10^8 cells/ml in buffer A.

(ii) Label the plasma membrane of cells using 10 μM *FAST* DiI (final concentration) or 8 μM (final concentration) $DiIC_{18}(3)$ in dark at ~25 °C with mild shaking in glass tubes for 30 min.
- In case of analysis of lateral diffusion of membrane proteins, skip **Step (ii)** and use a suitable strain expressing the fluorescently-tagged protein of interest (*see* **Note 3**).

(iii) Centrifuge and wash twice with buffer A.

(iv) Resuspend the cell pellet in 50 μl of buffer A.

(v) Transfer an aliquot of 10 μl of this suspension to a clean glass slide and mount between a glass slide and a poly-L-lysine pre-coated glass coverslip.

(vi) Seal the ends of the coverslip with nail enamel.

(c) *FRAP measurements.*

(i) FRAP measurements could be performed in an inverted confocal microscope equipped with high numerical aperture objective and suitable laser sources compatible with the fluorophore of interest. The choice of the laser excitation, dichroic mirrors, and emission filters is determined by the fluorophore used for a particular experiment. The choice of the objective lens, zoom factor, and pinhole settings would depend on the size of the cell and the thickness and size of the region of interest (ROI) being monitored. The detector gain could be changed in order to image cells with different protein expression levels or difference in labeling intensities. The detector gain

should be set to maximize the signal-to-noise ratio while avoiding saturation in any pixel (*see* **Note 4**).

- $DiIC_{18}(3)$ and *FAST* DiI could be excited using 543 nm line of a helium–neon laser (or 561 nm DPSS laser), and fluorescence emission could be collected using the 565–630 nm band-pass filter.
- GFP could be excited using 488 nm line of an argon laser, and fluorescence emission could be collected using the 500–550 nm band-pass filter.

(ii) Identify the cell of interest on the confocal microscope and bring it to the desired focus. Define a circular region of interest (ROI) of ~1 μm in radius which will be subsequently photobleached and monitored (*see* **Notes 5** and **6**).

(iii) The rule of thumb for any FRAP measurement is to achieve significant fluorescence photobleaching within a very short period of time. For successful photobleaching, high laser power with short bleach time should be chosen over low laser power with long bleach time (*see* **Note 7**). Theoretically, bleaching duration should be infinitesimally small compared to characteristic diffusion time (τ_d, the time required for half-maximal recovery of fluorescence). In reality, one could achieve ~70–80% photobleaching within ~100 ms using any modern confocal microscope.

(iv) Next, the photobleaching parameters (scan speed, laser power, and bleaching iterations) are determined empirically. The number of times (bleaching iterations) the laser scans the ROI to achieve significant extent of photobleaching is an important parameter. This number would depend on intrinsic factors such as mobility and photostability of the fluorophore for a given system, and on extrinsic factors such as laser power and scan speed of the laser beam. It is possible to use a different scan speed (with more number of bleaching iterations) during bleaching in order to achieve significant fluorescence photobleaching within a very short period of time. Typically, fluorescence in the bleach ROI should be reduced by 70–80% of the initial value in order to observe appreciable fluorescence recovery (*see* **Note 8**). Higher extents of photobleaching often induce artifacts in FRAP experiments since it could damage the sample or induce cross-linking of fluorophores (*see* **Note 9**).

(v) It is also necessary to avoid undesired photobleaching of the ROI while imaging (scanning) during pre- and post-bleach time points (*see* **Note 10**). Scanning laser power

should be set to the lowest possible power necessary for sufficient signal-to-noise of the fluorescence intensity over background (*see* **Note 10**). Typically, imaging parameters (dye concentration, laser power, and PMT voltage) should be adjusted in a way such that pre-bleach intensity is ~100 times more than background fluorescence.

(vi) Further optimization involves tuning imaging parameters (beam splitter configuration, emission bandpass, and pinhole diameters) to achieve an optimal collection of fluorescence and improving signal-to-noise ratio (*see* **Note 4**).

(vii) The next parameter is the total number of scans (sometimes referred to as cycles) to be acquired during the entire experiment (pre-bleach, bleach, and post-recovery). This number refers to the maximum number of scans before significant photobleaching of the sample becomes apparent (*see* **Note 11**).

(viii) The time interval between successive scans is then determined. This value is dependent on the recovery kinetics of the particular fluorophore being monitored. For molecules undergoing fast diffusion, the time interval would be small (or sometimes zero). In case of slow diffusion, the time interval between successive scans should be large (*see* **Note 12**). To ensure complete recovery of fluorescence after bleaching, it is generally advisable to monitor fluorescence recovery for a period of ~$4\tau_d$.

(ix) After standardizing the number of cycles (*see* points (vii) and (viii) above) to be acquired for the entire experiment, three separate phases of the FRAP measurement are performed. First, images are acquired with low-power laser settings to extract pre-bleach intensities. Typically, five to ten pre-bleach images are acquired before switching to the high-intensity laser pulse for selectively photobleaching the ROI in the shortest possible time. One must make sure that the pre-bleach fluorescence intensity of the sample, as well as the ROI, does not fluctuate significantly. Immediately after photobleaching, the sample is monitored using the same low-power imaging settings (as used for pre-bleach time points) until the required number of cycles is completed.

(x) Laser scanning confocal microscopes offer a number of options for data collection. These include image size (e.g., 512 × 512 or 1024 × 1024), range of data collection (8-bit or 12-bit), and different file formats. It is advised to determine the requirement of the image analysis software prior to data acquisition. Collect 20–30

recovery plots for each treatment condition and repeat the experiment at least on three different days.

(d) *Analysis of FRAP measurements.*

(i) Accurate analysis of FRAP data requires that the bleaching event is much shorter than the recovery time, and the recovery is monitored until a recovery plateau is achieved. After performing FRAP measurements, based on the protocol specified above, data representing the mean fluorescence intensity as a function of time are extracted from the ROI of each time series image (*see* **Note 13**). This data should be then background corrected by subtracting background fluorescence values collected by performing FRAP measurement on an area without cells.

(ii) The background-corrected fluorescence trace is then normalized to both the pre-bleach fluorescence intensity in the ROI and the time of bleach (*see* Fig. 3). The latter is achieved by subtracting the pre-bleach time from each data point on the time axis. This results in the pre-bleach time points starting from $t < 0$, bleach point $t = 0$, and first post-bleach time point starting from a time $t > 0$ (Fig. 3).

(iii) The normalized and background-subtracted fluorescence intensity in the ROI ($F(t)$) versus normalized time (t) is analyzed according to the uniform-disk illumination model based on theoretical framework given by [34]:

$$F(t) = [F(\infty) - F(0)]\,[\exp(-2\tau_d/t)(I_0(2\tau_d/t) + I_1(2\tau_d/t))] + F(0) \quad (1)$$

where $F(\infty)$ is the post-bleach recovered fluorescence at time $t \to \infty$, $F(0)$ is the bleached fluorescence intensity in the ROI immediately after bleach, and τ_d is the characteristic diffusion time. I_0 and I_1 are modified Bessel functions. We routinely perform nonlinear curve fitting of the recovery data to Eq. (1) using GraphPad Prism software version 4.0 (San Diego, CA).

- For FRAP data fitting using GraphPad Prism in the "equation type" tab, use the following equation:

  Y = (Fi-Fo)*(exp(−2*T/X)*(besseli(0,2*T/X) + besseli(1,2*T/X))) + Fo

  where Y is fluorescence intensity at time X; Fi = final fluorescence intensity; Fo = initial fluorescence intensity; and T = characteristic diffusion time (τ_d).

- Feed initial values of Fi, Fo, and T by looking at the fluorescence trace. For example, when analyzing the fluorescence recovery trace shown in Fig. 1, choose $Fi = 80$, $Fo = 20$, and $T = 12$.

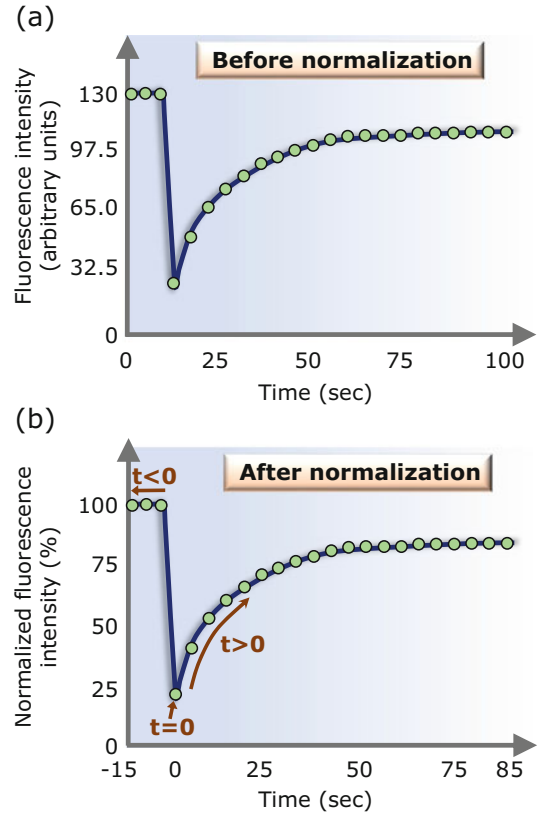

Fig. 3 Normalization of FRAP data. Raw data from FRAP measurements are normalized to both the pre-bleach fluorescence intensity in the ROI and the time of bleach. The latter is achieved by subtracting the total time until the first bleach point from each data point on the time axis. This results in the pre-bleach time points starting from $t < 0$, bleach point $t = 0$, and first post-bleach time point starting from a time $t > 0$

- The equation does not have a solution at $X = 0$. Therefore, remove the data point corresponding to $t = 0$.

(iv) Diffusion coefficient (D) is determined from the following equation:

$$D = \omega^2/4\tau_d \tag{2}$$

where ω is the radius of the ROI (*see* **Notes 14–17**).

(v) M_f is determined from the following equation:

$$M_f = [F(\infty) - F(0)]/[F(p) - F(0)] \tag{3}$$

where $F(p)$ is the mean background corrected and normalized pre-bleach fluorescence intensity, $F(\infty)$ is the post-bleach recovered

fluorescence at time $t \to \infty$, and $F(0)$ is the bleached fluorescence intensity in the ROI immediately after bleach. This ratio results in values between 0 and 1, or when expressed as a percentage, between 0% and 100% (*see* **Note 18**).

4 Notes

1. Light sensitive, store in a brown glass vial at −20 °C.
2. Clean coverslips with 70% ethanol (v/v) and air dry thoroughly.
3. Studying the dynamics of membrane proteins using FRAP requires fusion of a suitable fluorophore to the protein of interest. Desired characteristics for suitable fluorophores include (a) photostability during time-lapse imaging, (b) enough brightness to obtain a high signal-to-noise ratio, (c) absence of photoreversible bleaching, and (d) monomeric nature to avoid trivial association between tagged proteins. In this context, GFP-tagged (or its variants) proteins are ideal for use in FRAP measurements [22]. Additional advantages of GFP-tag include minimal photodamage to the cell during photobleaching [35]. The compact barrel-like structure of GFP shields the external environment from the damaging effects that are caused by the reactive intermediates generated during photobleaching [36–38].
4. It is crucial to adjust the acquisition parameters of the photomultiplier tube (PMT) in order to acquire images in the dynamic range of intensity acquisition. Pixel saturation (pixel intensity that exceeds the detector scale, e.g., >255 for an 8-bit image) during time series imaging would result in inaccurate estimation of the fluorescence recovery profile. This is because saturated pixels only record 255 as the intensity value and the true intensity of the pixel is not registered. The pinhole value, determined by the numerical aperture of the objective lens and the wavelength of the laser, should be kept constant across all images. The pinhole should be opened wide enough to acquire an adequate signal while keeping the laser intensity low to avoid photobleaching during pre- and post-bleach time points (*see* **Note 10**). It should be kept in mind that increasing the pinhole decreases the z resolution of the image by increasing the thickness of the optical section.
5. The bleach spot (ROI) should comprise a relatively small proportion of the cellular pool of fluorescent proteins. One should make sure that the dimension of the ROI is small compared to the size of the cell in order to limit the total loss of fluorescence,

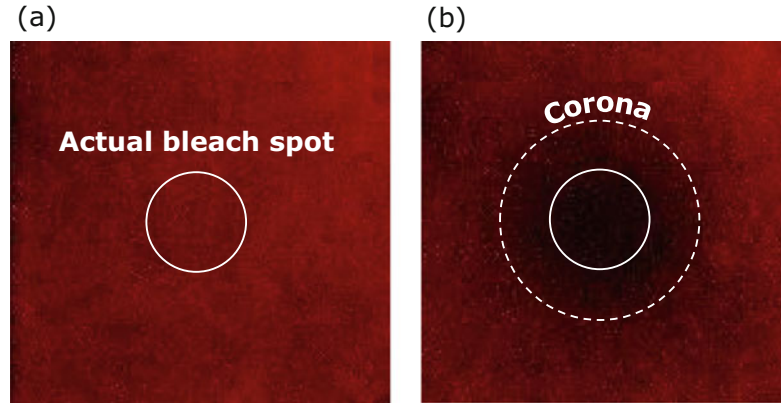

Fig. 4 The formation of a bleached "corona" due to prolonged bleaching in case of rapidly diffusing molecules. The bleach spot broadens with increasing bleaching iterations due to bleached "corona" (dashed circle) that emerges around the specified ROI (solid circle). This "corona" effect leads to a broadening of the bleached region beyond the marked ROI resulting in underestimation of diffusion coefficient

while it should be large enough to get a reasonable signal-to-noise ratio.

6. FRAP measurements are generally performed on the basal surface of cells that are in contact with the glass coverslip. This is because analysis of FRAP data is based on the theoretical framework which assumes that fluorescence recovery into the bleached area is isotropic in the plane of the membrane [34]. This condition is satisfied when one monitors the uniform fluorescent bottom surface of cells attached to the coverslip. In addition, the planar geometry of the uniform bottom surface of cells ensures that the theoretical dimensions of the circular ROI used for photobleaching are not distorted in the actual sample.
7. In case of a rapidly diffusing molecule, photobleaching cannot be assumed to be instantaneous. Since lateral diffusion does not "stop" while an ROI is photobleached, if photobleaching is slow relative to the diffusion of the molecule of interest, then the unbleached molecules will enter the ROI from the edges and become bleached. A longer bleach duration (of the same order of τ_d) would, therefore, result in the formation of a "corona" around the bleach spot [39] (*see* Fig. 4). This results in an effective increase in bleach spot radius and subsequently underestimates the value of diffusion coefficient. Experiments should be performed under conditions where the laser power is set to its maximum (100%) to achieve the shortest possible bleach period. For correction of the "corona" effect, please refer to **Note 14**.

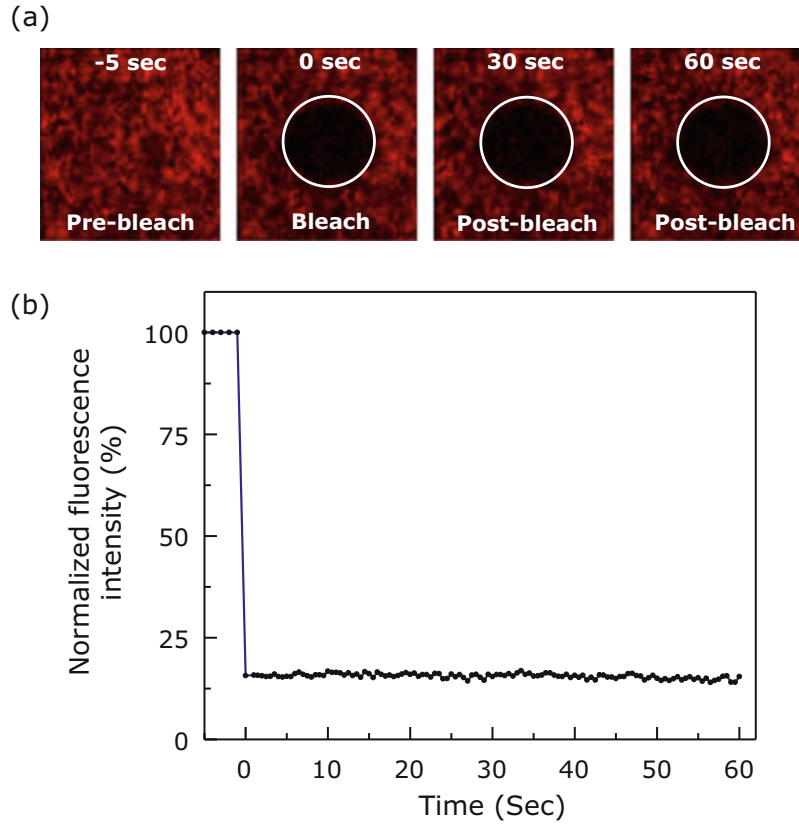

Fig. 5 Control experiments to check irreversibility of photobleaching. Reversibility of photobleaching could be monitored by bleaching a fixed sample using the identical imaging setup used for live samples. Panel (**a**) shows FRAP measurements performed on *FAST* DiI labeled plasma membrane of CHO-K1 cells that were fixed using 3.5% (v/v) formaldehyde. Panel (**b**) shows fluorescence recovery kinetics in the ROI (marked with a white circle in panel (**a**)). In absence of any reversible photobleaching, no fluorescence recovery should be observed

8. Photoreversible bleaching poses a problem during the quantitative analysis of FRAP data and could lead to an erroneous estimation of lateral diffusion [40, 41]. It is critical to establish conditions which confirm that bleaching is irreversible during the time course and condition of the experiment. To check for reversible photobleaching of the fluorophore in FRAP experiments, the bleaching conditions should be first standardized in fixed samples in which no recovery of fluorescence should be expected (*see* Fig. 5).
9. A simple test for photobleaching-induced immobile fractions due to crosslinking of fluorophores is to perform multiple FRAP measurements in the same region of interest in the same cell [42, 43] (Fig. 6). For such measurement, the diffusion coefficient should not change but the mobile fraction should be close to 100% in subsequent FRAP measurements

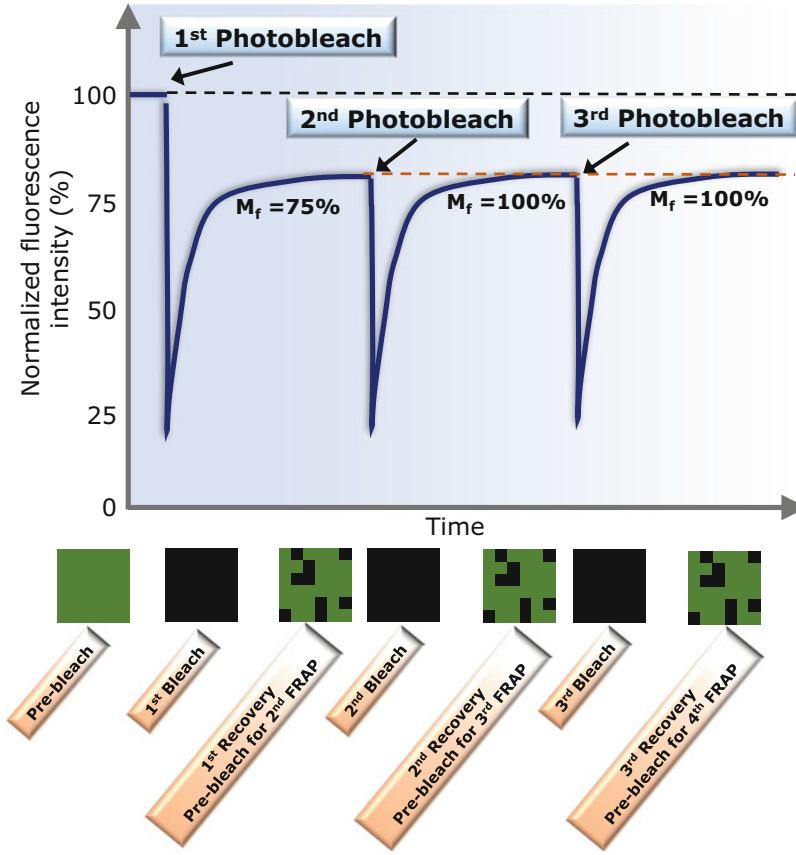

Fig. 6 Control experiments to check for photo-induced immobile fractions. A simple test for generation of photo-induced immobile fractions is to perform a second FRAP measurement in the same ROI in the same cell. In this example, the mobile fraction of the first FRAP experiment is ~75%. In the absence of photodamage-induced artifacts, complete fluorescence recovery should be observed from subsequent FRAP measurements in the same ROI. The bottom panel shows an illustration of time evolution of the bleach ROI during multiple photobleaching FRAP measurements. The black spots represent bleached fluorophores and the green spots represent unbleached fluorophores. In case of an ideal FRAP experiment, the post-recovery intensity after the second FRAP measurement should be the same as the pre-bleach intensity of the given FRAP measurement. A high recovery (~100%) during subsequent FRAP measurements indicates the actual "immobile" fraction, whereas reduced mobile fraction (comparable to first FRAP measurement) indicates potential photodamage and could lead to artifacts in data analysis

in the same ROI. As shown in Fig. 6, the mobile fraction of the first FRAP experiment is ~75%. In the absence of photodamage, 100% fluorescence recovery should be observed from second and subsequent FRAP measurements. The immobile molecules will be photobleached in the first FRAP and therefore would not contribute to the percent recovery observed in subsequent FRAP measurements. A lower value of mobile fraction (<100%) from subsequent FRAP experiments would

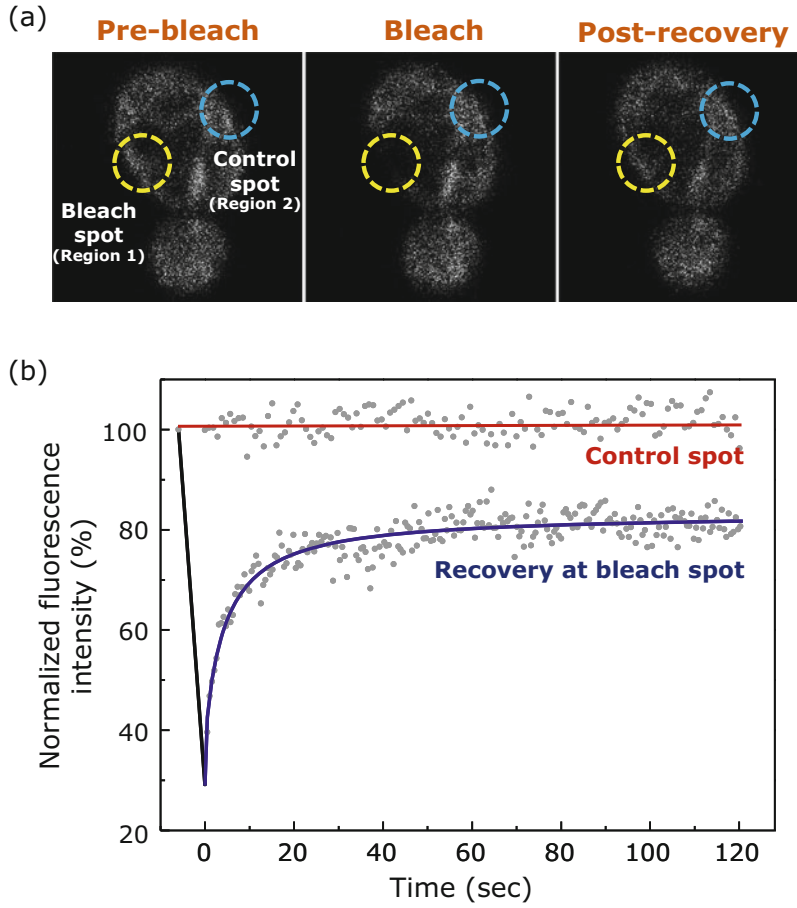

Fig. 7 A control experiment to check for photobleaching during imaging. (**a**) A representative FRAP experiment performed on *Candida* cells labeled with *FAST* DiI. The fluorescent periphery of cells representing the plasma membrane was selected for bleaching and monitoring recovery of fluorescence. Confocal images of the same cell before bleach (pre-bleach), immediately after bleach (bleach), and after recovery (post-recovery) for a representative FRAP experiment are shown in (**a**). Region 1 (bleach spot shown as yellow dashed line; radius = 1 μm) was monitored to measure fluorescence recovery after photobleaching; region 2 (control spot shown as blue dashed line) to detect any possible bleaching during scanning. Data representing the normalized mean fluorescence intensities from the regions depicted in (**a**) for the entire duration of the FRAP experiment are shown in (**b**). The relatively constant fluorescence intensity in the control spot (region 2) in (**b**) shows that the imaging conditions were optimized, and no significant photobleaching of fluorescence during time-lapse imaging took place. The solid lines are nonlinear regression fits of the data to Eq. (1). Adapted and modified with permission from [44]

indicate crosslinking-induced generation of immobile fluorophores.

10. A quick check to make sure that there is no photobleaching during imaging is to monitor the fluorescence intensity profile of a region away from the actual bleach spot (*see* Fig. 7). Fluorescence intensity of such a control spot should remain invariant with time. In a Zeiss LSM 510 meta confocal laser

scanning microscope, recommended condition for the acquisition of recovery time point with a 40 mW 488/514 nm argon laser line is 30–50% laser power with 0.1% to 2% transmission, for a specific pinhole (1 Airy unit).

11. In control experiments, a sample should be imaged using identical imaging settings without bleaching the ROI to find out the maximum number of scans possible before significant photobleaching of the sample. Let us assume that for a particular sample, photobleaching is observed after n number of scans (*see* Fig. 8). If such a sample has a slow rate of fluorescence recovery due to slow diffusion, a longer delay time (between two successive scans) should be given to capture the entire process of fluorescence recovery (till recovery reaches a plateau) within n number of scans (*see* Fig. 8).
12. In any FRAP measurement, it is crucial to capture the recovery of fluorescence intensity with highest possible temporal resolution. Currently, most of the commercially available laser scanning confocal microscopes are equipped with bidirectional scanning. Bidirectional scanning allows imaging the sample from both directions along the x-axis and significantly increases the scan rate. However, it is often necessary to adjust the phase shift correction to avoid image distortion. Additionally, line/frame averaging should be avoided while imaging as it slows down scan speed and leads to loss of time resolution between successive scans. For rapidly diffusing molecules where very high temporal resolution is required to capture the fluorescence recovery kinetics, it is advised to image the bleach ROI alone for rapid collection of data points. The only caveat of this approach is that the cell may shift in position during the course of time-lapse imaging, and this could induce further complication.
13. Discard fluorescence recovery traces that exhibit the following artifacts: (a) unstable pre-bleach fluorescence intensity, (b) recovery curves that do not display a plateau, (c) photobleaching during acquisition, and (d) fluctuations of fluorescence intensity due to cell movement (*see* Fig. 9).
14. Precise determination of the diffusion coefficient from a FRAP measurement depends strongly on how similar the dimension of the theoretical ROI (ω) is to the actual bleach spot dimension in the sample (since D has a square dependence on ω). The actual size of the bleach spot may not be same as the dimensions of the ROI for all experiments. If the bleach duration is long compared to τ_d, especially for confocal microscopes with relatively low-power laser and photostable fluorophore, the effective size of the bleach spot would depend on the duration of bleach. A longer bleach duration to obtain significant

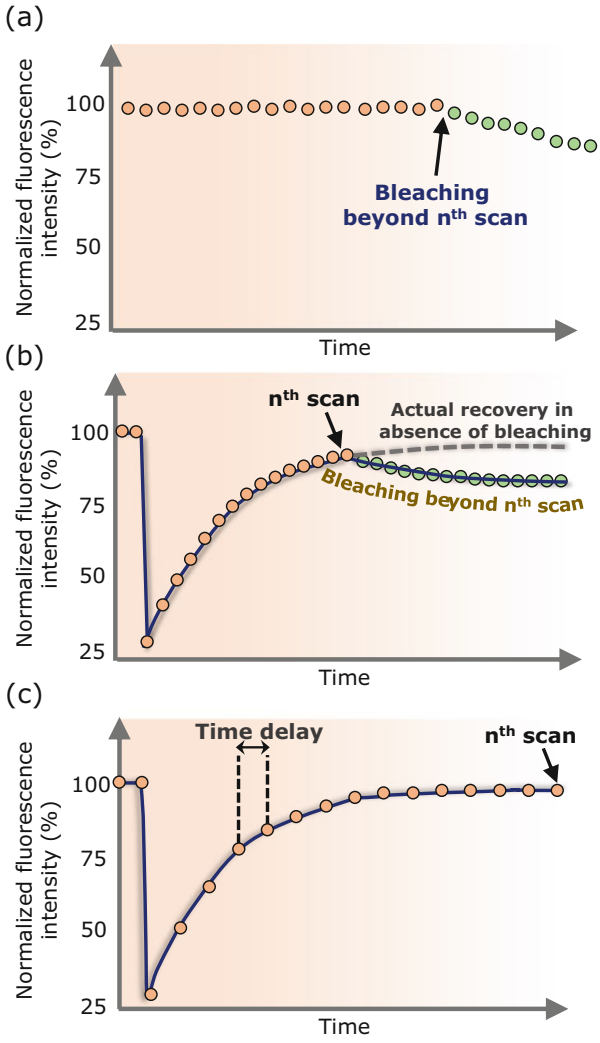

Fig. 8 Control experiment to minimize photobleaching during imaging. (**a**) A sample is imaged using identical imaging settings to be used for actual FRAP measurement, without bleaching the ROI. This would help to find out the maximum number of scans before significant photobleaching of the sample. Panel (**b**) shows that beyond *n*th scan, the post-bleach fluorescence recovery intensity is significantly affected by photobleaching. (**c**) A longer delay time (interval between two successive scans) should be given to capture the entire process of fluorescence recovery (till recovery reaches a plateau) within *n* scans

photobleaching in a sample with high diffusion tends to broaden the bleach spot (as shown in Fig. 4) leading to an underestimation of *D*. Fortunately, these estimates could be corrected to a significant extent by calculating the effective bleached spot size by relatively simple image analysis approaches previously described by us [45] (Fig. 10).

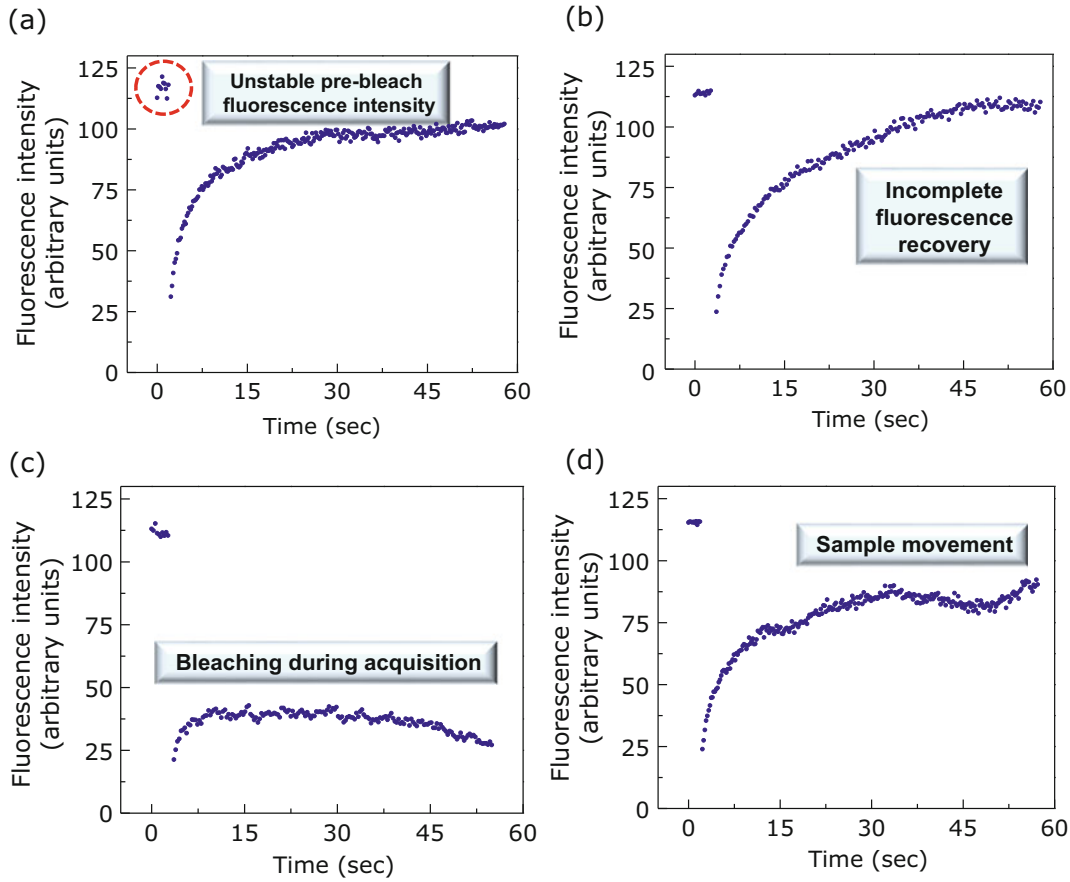

Fig. 9 Examples of raw FRAP data that should be discarded. Recovery curves (**a**) with unstable pre-bleach fluorescence intensity, (**b**) where fluorescence recovery is not complete and recovery plateau is not achieved, (**c**) with photobleaching during post-bleach acquisition, and (**d**) showing fluctuations in fluorescence intensity due to cell movement or drift of focus. Data from any of these cases should not be analyzed for calculation of diffusion parameters

15. Photobleaching using high laser illumination could lead to local heating of the sample as the laser power may reach ~1 mW/cm^2 [46, 47]. This could give rise to photo-induced crosslinking of molecules and significantly slow down diffusion. Such a phenomenon could be ruled out by performing the bleaching step using a range of laser powers. In the absence of any photo-induced crosslinking, D value should remain invariant over the range of laser powers used for photobleaching (*see* Fig. 11). A decrease in D value with higher laser power would indicate a reduction in the mobility of molecules due to the formation of higher molecular weight complex via crosslinking.
16. Equation (2) assumes unrestricted diffusion in a circular bleached ROI without any recovery from below or above the

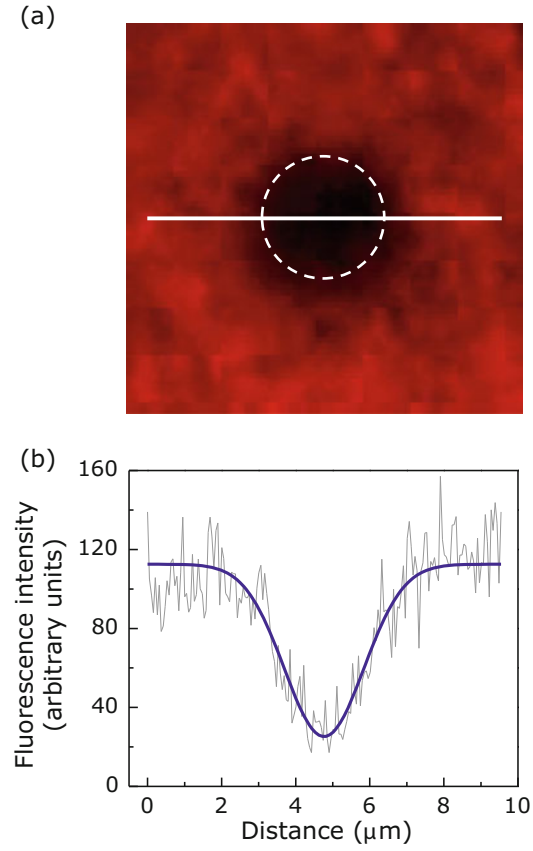

Fig. 10 Determination of actual bleach spot radius. Panel (**a**) represents the first acquired post-bleach image of *Candida* cell membrane stained with *FAST* DiI with an ROI of 1 μm radius. The fluorescence intensity profile along the straight line drawn across the bleached spot is represented in panel (**b**). The smooth line in panel (**b**) is a nonlinear regression fit of the data, and the noisy line represents a typical fluorescence intensity profile across the bleached spot. The half-width at half-maximum (HWHM) of the Gaussian amplitude function could be extracted to experimentally determine the actual bleach spot size

focal plane and is only valid for lateral diffusion in membranes [48].

17. The theoretical D of a protein is related to its size (mass) and its cellular environment. Deviations from this theoretical value could provide novel insight into the environment of the protein. If D is significantly lower than what is predicted based on the protein's mass, the protein could be incorporated in an aggregate or a large complex. In addition, the local environment of the protein could be significantly more viscous than expected. A third possibility could be that the protein could interact with a fixed scaffold such as the actin cytoskeleton [17, 49, 50]. On the other hand, if the lateral diffusion of a

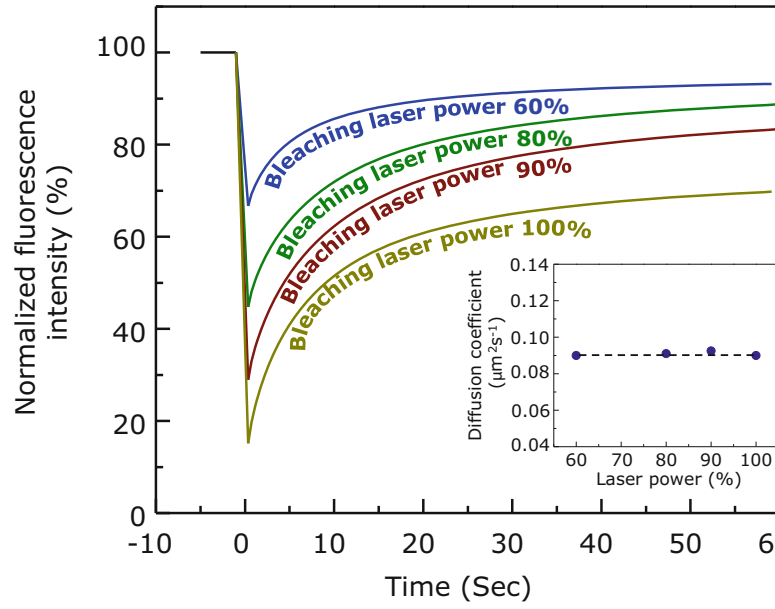

Fig. 11 A test for photo-induced crosslinking due to high bleaching laser power. Photobleaching using high laser illumination could lead to photo-induced crosslinking due to local heating and may slow down diffusion. Such a phenomenon should be ruled out by performing the bleaching step in FRAP measurements using a range of laser powers. The figure shows fitted fluorescence recovery curves to FRAP measurements performed in the same cell with a wide range of bleaching laser power. The inset shows the calculated value of the diffusion coefficient (D) for each of the fluorescence recovery curves. In absence of any photo-induced crosslinking, D value should remain invariant over the range of laser powers used for photobleaching

protein is faster than what is predicted, the protein might be undergoing directed transport via motor proteins or the local environment of the protein could be less viscous [51].

18. The mobile fraction (M_f) also reveals important information about protein dynamics. A decrease in M_f relative to control value indicates that the protein could be confined in compartments (domains) due to the formation of immobile aggregates by binding to a fixed/anchored substrate [52] and cannot contribute to fluorescence recovery. An increase in M_f would suggest that the protein is released from a fixed scaffold or exported out of a discontinuous compartment.

Acknowledgments

A.C. gratefully acknowledges support from SERB Distinguished Fellowship (Department of Science and Technology, Govt. of India). P.S. thanks the Council of Scientific and Industrial Research for the award of a Shyama Prasad Mukherjee Fellowship. A.C. is a Distinguished Visiting Professor at the Indian Institute of Technology Bombay (Mumbai), Adjunct Professor at the RMIT University (Melbourne, Australia), Tata Institute of Fundamental Research (Mumbai), and Indian Institute of Science Education and Research (Kolkata), and an Honorary Professor at the Jawaharlal Nehru Centre for Advanced Scientific Research (Bengaluru). We thank members of the Chattopadhyay laboratory for their comments and discussions.

Conflicts of Interest

There are no conflicts of interest to declare.

References

1. Edidin M (1994) Fluorescence photobleaching and recovery, FPR, in the analysis of membrane structure and dynamics. In: Damjanovich S, Edidin M, Szöllõsi J, Trón L (eds) Mobility and proximity in biological membranes. CRC, Boca Raton, pp 109–135
2. Lippincott-Schwartz J, Snapp E, Kenworthy A (2001) Studying protein dynamics in living cells. Nat Rev Mol Cell Biol 2:444–456
3. Kenworthy AK (2007) Fluorescence recovery after photobleaching studies of lipid rafts. In: McIntosh TJ (ed) Lipid Rafts, Methods in molecular biology, vol 398. Humana, Totowa, pp 179–192
4. Carisey A, Stroud M, Tsang R, Ballestrem C (2011) Fluorescence recovery after photobleaching. In: Wells CM, Parsons M (eds) Cell migration: developmental methods and protocols, Methods in molecular biology, vol 769. Humana, New York, pp 387–402
5. Jafurulla M, Chattopadhyay A (2015) Novel insights in membrane biology utilizing fluorescence recovery after photobleaching. Adv Exp Med Biol 842:27–40
6. Sarkar P, Chattopadhyay A (2019) Exploring membrane organization at varying spatiotemporal resolutions utilizing fluorescence-based approaches: implications in membrane biology. Phys Chem Chem Phys 21:11554–11563
7. Lippincott-Schwartz J, Snapp EL, Phair RD (2018) The development and enhancement of FRAP as a key tool for investigating protein dynamics. Biophys J 115:1146–1155
8. Poo M, Cone RA (1974) Lateral diffusion of rhodopsin in the photoreceptor membrane. Nature 247:438–441
9. Liebman PA, Entine G (1974) Lateral diffusion of visual pigment in photoreceptor disk membranes. Science 185:457–459
10. Peters R, Peters J, Tews KH, Bähr W (1974) A microfluorimetric study of translational diffusion in erythrocyte membranes. Biochim Biophys Acta 367:282–294
11. Axelrod D, Koppel DE, Schlessinger J, Elson E, Webb WW (1976) Mobility measurement by analysis of fluorescence photobleaching recovery kinetics. Biophys J 16:1055–1069
12. Jacobson K, Derzko Z, Wu E-S, Hou Y, Poste G (1976) Measurement of the lateral mobility of cell surface components in single, living cells by fluorescence recovery after photobleaching. J Supramol Struct 5:565(417)–576(428)
13. Chalfie M, Tu Y, Euskirchen G, Ward WW, Prasher DC (1994) Green fluorescent protein as a marker for gene expression. Science 263:802–805

14. Reits EAJ, Neefjes JJ (2001) From fixed to FRAP: measuring protein mobility and activity in living cells. Nat Cell Biol 3:E145–E147
15. Lagerholm BC, Weinreb GE, Jacobson K, Thompson NL (2005) Detecting microdomains in intact cell membranes. Annu Rev Phys Chem 56:309–336
16. Valdez-Taubas J, Pelham HRB (2003) Slow diffusion of proteins in the yeast plasma membrane allows polarity to be maintained by endocytic cycling. Curr Biol 13:1636–1640
17. Ganguly S, Pucadyil TJ, Chattopadhyay A (2008) Actin cytoskeleton-dependent dynamics of the human serotonin$_{1A}$ receptor correlates with receptor signaling. Biophys J 95:451–463
18. Tsien RY (1998) The green fluorescent protein. Annu Rev Biochem 67:509–544
19. White J, Stelzer E (1999) Photobleaching GFP reveals protein dynamics inside live cells. Trends Cell Biol 9:61–65
20. Lippincott-Schwartz J, Patterson GH (2003) Development and use of fluorescent protein markers in living cells. Science 300:87–91
21. Haldar S, Chattopadhyay A (2009) Green fluorescent protein: the molecular lantern that illuminates the cellular interior. J Biosci 34:169–172
22. Sarkar P, Chattopadhyay A (2018) GFP fluorescence: a few lesser-known nuggets that make it work. J Biosci 43:421–430
23. Fucile S, Palma E, Martínez-Torres A, Miledi R, Eusebi F (2002) The single-channel properties of human acetylcholine α7 receptors are altered by fusing α7 to the green fluorescent protein. Proc Natl Acad Sci USA 99:3956–3961
24. Saffman PG, Delbrück M (1975) Brownian motion in biological membranes. Proc Natl Acad Sci USA 72:3111–3113
25. Maekawa M, Fairn GD (2014) Molecular probes to visualize the location, organization and dynamics of lipids. J Cell Sci 127:4801–4812
26. Klymchenko AS, Kreder R (2014) Fluorescent probes for lipid rafts: from model membranes to living cells. Chem Biol 21:97–113
27. Klausner RD, Wolf DE (1980) Selectivity of fluorescent lipid analogues for lipid domains. Biochemistry 19:6199–6203
28. Spink CH, Yeager MD, Feigenson GW (1990) Partitioning behavior of indocarbocyanine probes between coexisting gel and fluid phases in model membranes. Biochim Biophys Acta 1023:25–33
29. Kalipatnapu S, Chattopadhyay A (2004) A GFP fluorescence-based approach to determine detergent insolubility of the human serotonin$_{1A}$ receptor. FEBS Lett 576:455–460
30. Baumgart T, Hunt G, Farkas ER, Webb WW, Feigenson GW (2007) Fluorescence probe partitioning between L_o/L_d phases in lipid membranes. Biochim Biophys Acta 1768:2182–2194
31. Mukherjee S, Soe TT, Maxfield FR (1999) Endocytic sorting of lipid analogues differing solely in the chemistry of their hydrophobic tails. J Cell Biol 144:1271–1284
32. Pucadyil TJ, Chattopadhyay A (2006) Effect of cholesterol on lateral diffusion of fluorescent lipid probes in native hippocampal membranes. Chem Phys Lipids 143:11–21
33. Mukhopadhyay K, Prasad T, Saini P, Pucadyil TJ, Chattopadhyay A, Prasad R (2004) Membrane sphingolipid-ergosterol interactions are important determinants of multidrug resistance in *Candida albicans*. Antimicrob Agents Chemother 48:1778–1787
34. Soumpasis DM (1983) Theoretical analysis of fluorescence photobleaching recovery experiments. Biophys J 41:95–97
35. Lippincott-Schwartz J, Presley JF, Zaal KJM, Hirschberg K, Miller CD, Ellenberg J (1999) Monitoring the dynamics and mobility of membrane proteins tagged with green fluorescent protein. Methods Cell Biol 58:261–281
36. Yang F, Moss LG, Phillips GN Jr (1996) The molecular structure of green fluorescent protein. Nat Biotechnol 14:1246–1251
37. Prendergast FG (1999) Biophysics of the green fluorescent protein. Methods Cell Biol 58:1–18
38. Haldar S, Chattopadhyay A (2007) Dipolar relaxation within the protein matrix of the green fluorescent protein: a red edge excitation shift study. J Phys Chem B 111:14436–14439
39. Weiss M (2004) Challenges and artifacts in quantitative photobleaching experiments. Traffic 5:662–671
40. Dickson RM, Cubitt AB, Tsien RY, Moerner WE (1997) On/off blinking and switching behaviour of single molecules of green fluorescent protein. Nature 388:355–358
41. McAnaney TB, Zeng W, Doe CFE, Bhanji N, Wakelin S, Pearson DS, Abbyad P, Shi X, Boxer SG, Bagshaw CR (2005) Protonation, photobleaching, and photoactivation of yellow fluorescent protein (YFP 10C): a unifying mechanism. Biochemistry 44:5510–5524
42. Lippincott-Schwartz J, Altan-Bonnet N, Patterson GH (2003) Photobleaching and

photoactivation: following protein dynamics in living cells. Nat Cell Biol 5:S7–S14

43. Snapp EL, Altan N, Lippincott-Schwartz J (2003) Measuring protein mobility by photobleaching GFP chimeras in living cells. Curr Prot Cell Biol 21(1):1–21.1.24
44. Khandelwal NK, Sarkar P, Gaur NA, Chattopadhyay A, Prasad R (2018) Phosphatidylserine decarboxylase governs plasma membrane fluidity and impacts drug susceptibilities of *Candida albicans* cells. Biochim Biophys Acta 1860:2308–2319
45. Pucadyil TJ, Chattopadhyay A (2006) Confocal fluorescence recovery after photobleaching of green fluorescent protein in solution. J Fluoresc 16:87–94
46. Axelrod D (1977) Cell surface heating during fluorescence photobleaching recovery experiments. Biophys J 18:129–131
47. De Los SC, Chang C-W, Mycek M-A, Cardullo RA (2015) FRAP, FLIM, and FRET: detection and analysis of cellular dynamics on a molecular scale using fluorescence microscopy. Mol Reprod Dev 82:587–604
48. Koppel DE, Sheetz MP, Schindler M (1980) Lateral diffusion in biological membranes. A normal-mode analysis of diffusion on a spherical surface. Biophys J 30:187–192
49. Pucadyil TJ, Chattopadhyay A (2007) Cholesterol depletion induces dynamic confinement of the G-protein coupled serotonin$_{1A}$ receptor in the plasma membrane of living cells. Biochim Biophys Acta 1768:655–668
50. Ganguly S, Chattopadhyay A (2010) Cholesterol depletion mimics the effect of cytoskeletal destabilization on membrane dynamics of the serotonin$_{1A}$ receptor: a zFCS study. Biophys J 99:1397–1407
51. Kreutzberger AJB, Ji M, Aaron J, Mihaljević L, Urban S (2019) Rhomboid distorts lipids to break the viscosity-imposed speed limit of membrane diffusion. Science 363:eaao0076
52. Feder TJ, Brust-Mascher I, Slattery JP, Baird B, Webb WW (1996) Constrained diffusion or immobile fraction on cell surfaces: a new interpretation. Biophys J 70:2767–2773